Supporting Information

The Pro33 variant (HPA-1b) of $\alpha_{IIb}\beta_3$ allosterically shifts the dynamic conformational equilibrium of the integrin towards an active state

Giulia Pagani[1], Joana P. V. Pereira[2§], Volker R. Stoldt[2§], Andreas Beck[3], Rüdiger E. Scharf[2,4#], Holger Gohlke[1,5#*]

[1]Institute for Pharmaceutical and Medicinal Chemistry, Heinrich Heine University Düsseldorf, Düsseldorf, Germany

[2]Division of Experimental and Clinical Hemostasis, Hemotherapy and Transfusion Medicine, Institute of Transplantation Diagnostics and Cell Therapeutics, Heinrich Heine University Düsseldorf Medical Center, Düsseldorf, Germany

[3]Institute of Informatics, Heinrich Heine University Düsseldorf, Düsseldorf, Germany

[4]Biological Medical Research Center, Heinrich Heine University Düsseldorf, Düsseldorf, Germany

[5]John von Neumann Institute for Computing (NIC), Jülich Supercomputing Centre (JSC) & Institute for Complex Systems - Structural Biochemistry (ICS 6), Forschungszentrum Jülich GmbH, Jülich, Germany

[§]Current affiliation: Dept. of General, Visceral and Pediatric Surgery, Heinrich Heine University Medical Center & Faculty of Medicine, Heinrich Heine University Düsseldorf, Düsseldorf, Germany

[#]Share senior authorship

[*]Address: Universitätsstr. 1, D-40225 Düsseldorf, Germany.

Phone: (+49) 211 81 13662; Fax: (+49) 211 81 13847

E-mail: gohlke@uni-duesseldorf.de or h.gohlke@fz-juelich.de

Table of Contents

Supplemental Methods

Determination of HPA-1 alleles of $\alpha_{IIb}\beta_3$ and α_2 C807T genotypes of $\alpha_2\beta_1$

Prior to blood collection for this study, genotyping of HPA-1 and α_2C807T had been performed. Genomic DNA was extracted from whole blood using the QIAmp blood kit (Qiagen, Hilden, Germany). Upon amplification by polymerase chain reaction, genotypes were determined by allele-specific restriction enzyme analysis (1). The results of genotyping were confirmed by a second analysis using the LightCycler™ system (Roche Diagnostics, Mannheim, Germany) (2) and the results of both procedures were in 100% concordance.

Donor population

Homozygous carriers of either allele, Leu33 (HPA-1a) or Pro33 (HPA-1b), which did not carry the $\alpha_2$807CT or $\alpha_2$807TT genotype of $\alpha_2\beta_1$, were selected for the subsequent experiments. Group A (HPA-1a/1a) consisted of 8 individuals (5 males, 3 females, mean age: 38.8 yrs., range: 21 to 58 yrs.); group B consisted of 7 individuals (4 males, 3 females, mean age: 45.3 yrs., range: 35 to 54 yrs.).

Compounds

Abciximab 4µg/ml (c7E3, ReoPro, Centocor, Inc/Eli Lilly, Indianapolis, IN, USA) is a murine-human chimeric monoclonal antibody fragment directed against human $\alpha_{IIb}\beta_3$. A complex-specific anti-$\alpha_{IIb}\beta_3$ antibody, anti-CD41 (clone MEM-06, Exbio, Praha, Czech Republic) was used for flow cytometric analysis of transfected HEK293 cells. For calibration of the flow cytometer and quantitation of $\alpha_{IIb}\beta_3$ expression, fluorescent microspheres (F-36905, Molecular Probes, Eugene, OR, USA) were used.

Design and construction of plasmids

Two plasmids were generated first by cloning the cDNA of the α_{IIb} human integrin gene (ITGA2B), a gift from Dr. S. Shattil (University of California, San Diego, CA, USA), and the cDNA of the β_3 human integrin gene (ITGB3), a gift from Dr. J. Jones (Northwestern University Medical School, Chicago, IL, USA), downstream the cytomegalovirus promoter in the pcDNA3.1(-) plasmid (Thermo Fisher, formerly Invitrogen, Waltham, MA, USA). A third plasmid, containing the Pro-for-Leu substitution in the β_3 subunit was generated by site-directed mutagenesis, as reported by Kunkel (3). Subsequently, the coding sequence of mVenus (plasmid # 27794), a gift from S. Vogel (Addgene, Cambridge, MA, USA) was cloned downstream the α_{IIb} coding sequence, and the coding sequence of mCherry (Clontech Laboratories, Takara Bio, Mountain View, CA, USA) was cloned downstream the β_3Leu33 and β_3Pro33 coding sequences in the respective plasmids. In initial fusion constructs, the length of the linker between the C-terminus of each subunit and the N-terminus of the corresponding fluorescent protein (mVenus or mCherry) was varied (4), and combinations of these constructs were tested in transiently transfected HEK293 cell by acceptor-photobleaching to determine optimal basal FRET efficiency. Accordingly, the construct containing a linker of 39 amino acids between α_{IIb} (C-terminus) and mVenus (N-terminus),

and a linker of 6 amino acids between β_3Leu33 or β_3Pro33 (C-terminus) and mCherry (N-terminus), was chosen.

Importantly, mVenus and mCherry coding sequences were cloned in frame with the integrin subunits coding sequences with removal of the original stop codon of the integrin subunits (4) for expression as fusion proteins. The sequences of the three resulting plasmids were confirmed by Sanger sequencing (Biological Medical Research Center, Heinrich Heine University Düsseldorf), using the primers listed in **Tables S1** and **S2**.

Cell line culture and transfection

HEK293 cells were purchased from the Leibniz Institute DSMZ - German Collection of Microorganisms and Cell Cultures (DSMZ, Braunschweig, Germany) and cultured according to the recommended conditions (DMEM supplemented with 10% of fetal bovine serum (FBS) and 1% penicillin-streptomycin (PCN-STR). DMEM, FBS, and PCN-STR were obtained from Thermo Fischer Scientific (Waltham, MA, USA). To achieve expression of the complete $\alpha_{IIb}\beta_3$ receptor complex of either isoform, Leu33 (HPA-1a) or Pro33 (HPA-1b), in HEK293 cells, a double transient transfection was performed with the plasmids α_{IIb}mVenus and β_3Leu33mCherry or β_3Pro33mCherry, respectively. HEK293 cells transfected with an empty vector DNA were used as controls in the flow cytometry analyses, and cells double transfected with αIIbmVenus and β_3Leu33 or β_3Pro33 plasmids (without mCherry) served as controls in FRET-APB experiments. The transfection protocol was performed using the Effectene® Transfection Reagent (Qiagen, Hilden, Germany). 24 h prior to transfection, $1.6x10^5$ cells were seeded on a 6-well plate (Greiner Bio-one, Frickenhausen, Germany) in culture medium. On the next day, 0.4 µg of integrin α_{IIb} encoding plasmid and 0.4 µg of each β_3 encoding plasmids were diluted in EC (Enhancer and DNA condensation) buffer (total final volume of 100 µl), 3.2 µl of transfection enhancer was added and the mixture incubated

at RT for 5 min. Subsequently, 10 µl of Effectene® was added and the mixture incubated at RT for 10 min. Finally, 200 µl of cell culture medium was added, and the mixture was carefully pipetted into the wells containing the cells. 24 h after transfection, the medium was replaced by standard cell culture medium (DMEM supplemented with 10% FBS and 1% PCN-STR).

Image acquisition was achieved by using the Metamorph Software (v. 7.7.7.0), and image processing was performed with Adobe Photoshop CS3 (Adobe, USA) software.

FRET acceptor-photobleaching (APB) analyses

mVenus fluorescence intensity measured in the ROI varied between 11 and 134 (mean ± SEM, 37.85±1.992) for cells transfected with α_{IIb}mVenus and β_3Leu33mCherry plasmids and between 7 and 93 (35.27 ± 2.048) for cells transfected with αIIbmVenus and β3Pro33mCherry plasmids, respectively; mCherry fluorescence intensity varied between 12 and 120 (54.37 ± 2.284) for cells transfected with α_{IIb}mVenus and β_3Leu33mCherry plasmids and between 12 and 99 (44.90 ± 2.159) for cells transfected with α_{IIb}mVenus and β_3Pro33mCherry plasmids. Transfected cells were randomly chosen for analysis.

Supplemental Tables

Table S1: Primers for α_{IIb}mVenus.

T7minus1	AATACGACTCACTATAGGG
Seq-p101-I	TGGGACAAGCGTTACTGTG
Seq-p101-II	GACCGGGATGGCTACAATG
Seq-p101-III	TCGAGATGAGGCAGACTTC
Seq-p101-IV	CAGCAGAAGAAGGTGAGAG
Seq-p101-mVenus	GGCAACTAGAAGGCACAGTC
RPC	ACAGCTATGACCATGATTACG
Seq-p101-Hyg-fw	ACAGCTATGACCATGATTACG
pEGFP-RP	AACAGCTCCTCGCCCTTG

Table S2: Primers for β_3mCherry.

pEGFP-FP	TTTAGTGAACCGTCAGATC
Seq-p106-I	CTTGCCCATGTTTGGCTAC
Seq-p106-II	GGCCTCAAGTCTTGTATGG
Seq-p106-III	TGGCAGCTGTGTCTGTATC
pEGFP_C2-RP	TTTAAAGCAAGTAAAACCTC
Seq-p106-Zeo	GAACAAACGACCCAACAC

Table S3: Local geometry of the metal ion binding sites.

	Leu33 (HPA-1a) isoform			Pro33 (HPA-1b) isoform		
	SimI[a]	**SimII**[a]	**SimIII**[a]	**SimI**[a]	**SimII**[a]	**SimIII**[a]
SyMBS···P219$_O$	2.03±0.00	2.02±0.00	2.02±0.00	2.03±0.01	2.05±0.01	2.02±0.00
	2.05±0.01[b]			2.03±0.01[b]		
SyMBS···E220$_{oε1}$	1.95±0.00	1.96±0.00	1.95±0.00	1.05±0.004	1.95±0.00	1.94±0.002
	1.95±0.00[b]			1.95±0.01[b]		
MIDAS···E220$_{oε2}$	4.02±0.01	4.06±0.00	4.07±0.01	4.00±0.01	4.01±0.03	4.09±0.00
	4.05±0.01[b]			4.03±0.04[b]		
MIDAS···D119$_{oδ2}$	1.99±0.00	2.00+0.01	1.99±0.01	2.03±0.007	2.04±0.05	1.99±0.00
	1.99±0.01[b]			2.02±0.05[b]		
AMIDAS···D126$_{oδ1}$	2.07±0.01	2.14±0.02	2.17±0.02	2.35±0.04	1.95±0.00	2.81±0.05
	2.13±0.04[b]				2.37±0.07[b]	
AMIDAS···D127$_{oδ1}$	1.95±0.00	1.95±0.00	1.95±0.01	2.28±0.29	2.58±0.10	1.95±0.00
	1.95±0.01[b]			2.27±0.31[b]		

[a] Mean value and SEM, in Å, calculated for each MD simulation.
[b] Mean value and SEM, in Å, calculated across three MD simulations.

Table S4: RMSD of $\alpha_{IIb}\beta_3$ domains after domain-wise alignment.

		Leu33 (HPA-1a) isoform			Pro33 (HPA-1b) isoform		
	Domain	**Sim I[a]**	**Sim II[a]**	**Sim III[a]**	**Sim I[a]**	**Sim II[a]**	**Sim III[a]**
Sub α_{IIb}	**β-propeller**	1.71±0.01	2.04±0.04	1.91±0.01	2.33±0.03	1.94±0.01	2.17±0.01
		1.89±0.04[b]			2.15±0.0[b]3		
	thigh	1.86±0.05	1.99±0.13	1.95±0.03	1.75±0.02	1.78±0.04	1.82±0.03
		1.94±0.14[b]			1.78±0.06[b]		
	calf-1	1.71±0.12	2.39±0.03	2.16±2.09	2.15±0.10	1.89±0.02	1.86±0.07
		2.09±0.13[b]			1.78±0.12[b]		
	calf-2	1.85±0.16	2.56±0.13	1.43±0.01	3.39±0.12	2.15±0.14	2.02±0.03
		1.95±0.13[b]			2.52±0.19[b]		
Sub β_3	**βA**	2.37±0.03	1.43±0.01	2.06±0.07	1.50±0.05	1.63±0.01	2.65±0.01
		1.96±0.07[b]			1.92±0.05[b]		
	hybrid	2.60±0.15	2.56±0.02	2.63±0.05	2.91±0.03	2.59±0.05	2.69±0.08
		2.51±0.16[b]			2.73±0.10[b]		
	PSI	1.60±0.03	1.62±0.03	1.60±0.02	1.72±0.03	3.97±0.07	1.61±0.04
		1.60±0.05[b]			2.43±0.09[b]		
	EGFs	2.58±0.03	2.44±0.09	2.33±0.23	3.31±0.04	4.23±0.08	3.89±0.06
		2.45±0.25[b]			3.81±0.09[b]		
	β-tail	4.55±0.03	5.96±0.09	4.26±0.04	4.24±0.17	4.91±0.04	4.43±0.03
		4.93±0.11[b]			4.53±0.17[b]		

[a] Mean value and SEM, in Å, calculated for each MD simulation.
[b] Mean value and SEM, in Å, calculated across three MD simulations.

Table S5: RMSD of the $\alpha_{IIb}\beta_3$ integrin domains after alignment of the head region.

		Leu33 (HPA-1a) isoform			Pro33 (HPA-1b) isoform		
	Domain	**Sim I[a]**	**Sim II[a]**	**Sim III[a]**	**Sim I[a]**	**Sim II[a]**	**Sim III[a]**
Sub α_{IIb}	**β-propeller**	2.82±0.37	2.53±0.03	2.27±0.07	2.71±0.03	2.34±0.02	2.74±0.04
		2.54±0.37[b]			2.60±0.06[b]		
	thigh	5.70±0.09	5.41±0.34	6.64±0.11	9.84±0.15	10.75±1.11	8.45±0.45
		5.91±0.37[b]			9.68±1.20[b]		
	calf-1	7.48±0.85	5.79±0.41	8.61±0.37	10.73±0.08	12.79±0.52	11.31±0.49
		7.90±1.02[b]			11.61±0.72[b]		
	calf-2	8.93±0.44	8.18±0.74	11.39±0.19	13.25±0.24	16.35±0.38	21.13±2.65
		9.50±0.89[b]			16.91±2.69[b]		
Sub β_3	**βA**	4.00±0.30	2.75±0.15	2.91±0.06	2.39±0.11	2.35±0.04	3.34±0.05
		3.22±0.34[b]			2.70±0.13[b]		
	hybrid	6.49±0.61	7.62±0.26	8.21±0.05	5.66±0.12	8.36±0.31	6.52±0.22
		7.29±0.67[b]			6.85±0.40[b]		
	PSI	11.72±0.82	12.03±0.30	12.53±1.98	10.82±0.15	18.15±0.79	6.58±0.600
		12.09±2.16[b]			11.85±1.01[b]		
	EGFs	9.25±0.97	10.03±1.34	9.77±0.67	9.89±0.09	14.41±0.70	8.40±0.21
		9.68±1.78[b]			10.73±0.73[b]		
	β-tail	17.10±0.21	7.87±0.50	19.55±0.34	7.88±0.15	19.30±0.12	16.65±0.46
		14.83±0.64[b]			14.61±0.50[b]		

[a] Mean value and SEM, in Å, of the C_α atom RMSD of $\alpha_{IIb}\beta_3$ domains with respect to the starting structure after a mass-weighted alignment onto the β-propeller and βA domains, calculated for each MD simulation.
[b] Mean value and SEM, in Å, of the C_α atom RMSD of $\alpha_{IIb}\beta_3$ domains with respect to the starting structure after a mass-weighted alignment onto the β-propeller and βA domains, calculated across three MD simulations.

Table S6: RMSD and R_g of $\alpha_{IIb}\beta_3$.

	Leu33 (HPA-1a) isoform			Pro33 (HPA-1b) isoform		
	SimI[a]	**SimII**[a]	**SimIII**[a]	**SimI**[a]	**SimII**[a]	**SimIII**[a]
RMSD_ALL	6.76±0.41	5.68±0.54	7.46±0.47	7.55±0.07	10.40±0.30	9.55±0.14
	6.64±0.83[b]			9.17±0.34[b]		
	** [c]					
Rg_ALL	39.75±0.04	39.68±0.08	39.39±0.02	40.04±0.03	39.67±0.05	41.25±0.21
	39.61±0.09[b]			40.32±0.22[b]		
	* [c]					

[a] Mean value and SEM, in Å, calculated for each MD simulation.
[b] Mean value and SEM, in Å, calculated across three MD simulations.
[c] *: p <0.05, **: p < 0.001, ***: p < 0.0001 (according to the t-test for parametric testing).

Table S7: Kink, bending, and splaying angles.

	Leu33 (HPA-1a) isoform			Pro33 (HPA-1b) isoform		
	SimI[a]	**SimII**[a]	**SimIII**[a]	**SimI**[a]	**SimII**[a]	**SimIII**[a]
Kink[°]	137.38±2.33	136.99±1.43	139.55±0.36	140.02±0.56	154.06±1.35	165.25±0.35
	137.97±2.76[b]			153.11±1.50[b]		
	*** [c]					
Bending[°]	45.91±1.30	42.92±0.45	38.64±0.11	48.82±0.45	44.78±0.33	54.92±1.66
	42.49±1.38[b]			48.74±1.75[b]		
	* [c]					
Splaying[°]	22.85±0.15	27.16±0.13	24.05±0.06	26.88±0.08	28.65±0.44	27.76±0.08
	24.69±0.21[b]			27.76±0.45[b]		
	*** [c]					

[a] Mean value and SEM, in °, calculated for each MD simulation.
[b] Mean value and SEM, in °, calculated across three MD simulations.
[c] *: p <0.05, **: p < 0.001, ***: p < 0.0001 (according to the t-test for parametric testing).

Table S8: Distance between the N-terminus and C-terminus.

	Leu33 (HPA-1a) isoform			Pro33 (HPA-1b) isoform		
	SimI[a]	**SimII**[a]	**SimIII**[a]	**SimI**[a]	**SimII**[a]	**SimIII**[a]
βA···β-tail	35.70±0.33	40.81±0.52	31.30±0.05	43.45±0.24	42.86±1.51	47.95±0.75
	35.94±0.62			44.76±1.70		
	***					
calf-2···β-tail	29.65±0.10	28.31±0.55	25.92±0.03	29.03±0.08	31.00±0.22	28.17±0.04
	27.95±0.56			29.40±0.24		
	*					
calf-2···β-propeller	53.54±0.47	53.87±0.51	52.81±0.28	57.21±0.27	52.58±0.10	65.75±1.42
	53.07±0.75			58.51±1.45		
	*** [c]					

[a] Mean value and SEM, in Å, calculated for each MD simulation.
[b] Mean value and SEM, in Å, calculated across three MD simulations.
[c] *: p <0.05, **: p < 0.001, ***: p < 0.0001 (according to the t-test for parametric testing).

Table S9: Distance at the interface between PSI and the EGF-1/EGF-2 domains

	Leu33 (HPA-1a) isoform			Pro33 (HPA-1b) isoform		
	SimI[a]	**SimII**[a]	**SimIII**[a]	**SimI**[a]	**SimII**[a]	**SimIII**[a]
L33P···S469	7.32±0.28	8.45±0.10	8.59±0.28	12.60±0.21	11.49±0.47	11.34±0.60
	8.12±0.40			11.81±0.79		
	*					
L33P···Q481	6.45±0.28	6.63±0.35	6.77±0.24	13.75±0.21	10.03±0.54	13.38±0.84
	6.65±0.37			12.38±1.02		
	***					

[a] Mean value and SEM, in Å, calculated for each MD simulation.
[b] Mean value and SEM, in Å, calculated across three MD simulations.
[c] *: p <0.05, **: p < 0.001, ***: p < 0.0001 (according to the *t*-test for parametric testing).

Table S10: Native and non-native contacts involving the AB loop

	Leu33 (HPA-1a) isoform			Pro33 (HPA-1b) isoform		
	SimI[a]	**SimII**[a]	**SimIII**[a]	**SimI**[a]	**SimII**[a]	**SimIII**[a]
Native	374±4	279±7	357±4	295±6	247±4	301±2
	336±9			281±6		
	***					
Non-Native	869±13	977±13	726±32	191±6	538±9	436±37
	857±37			388±39		
	***					

[a] Mean value and SEM calculated for each MD simulation.
[b] Mean value and SEM calculated across three MD simulations.
[c] *: p <0.05, **: p < 0.001, ***: p < 0.0001 (according to the *t*-test for parametric testing).

Supplemental Figures

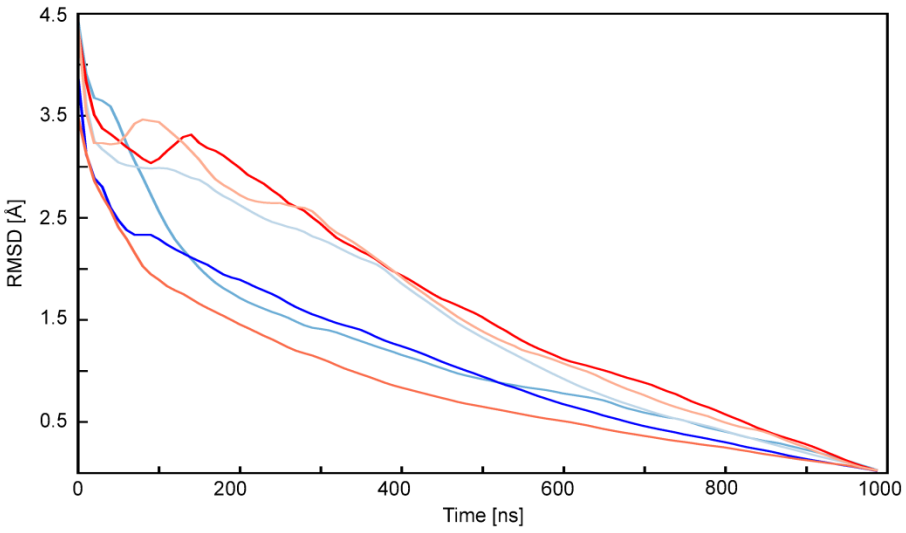

Fig. S1: RMSD average correlation.

RMSD average correlation (RAC) computed for the three independent MD simulations of $\alpha_{IIb}\beta_3$ expressing Leu33 (HPA-1a) (colored in three different shades of blue) or Pro33 (HPA-1b) (colored in three different shades of red) isoforms, respectively, as described in ref. (5). The structures were mass-weighted fitted on the C_α atoms of the head part (propeller domain and βA domain), excluding the first 200 ns from the trajectories, applying an offset of 250 frames, and using as reference the running average calculated over each time interval.

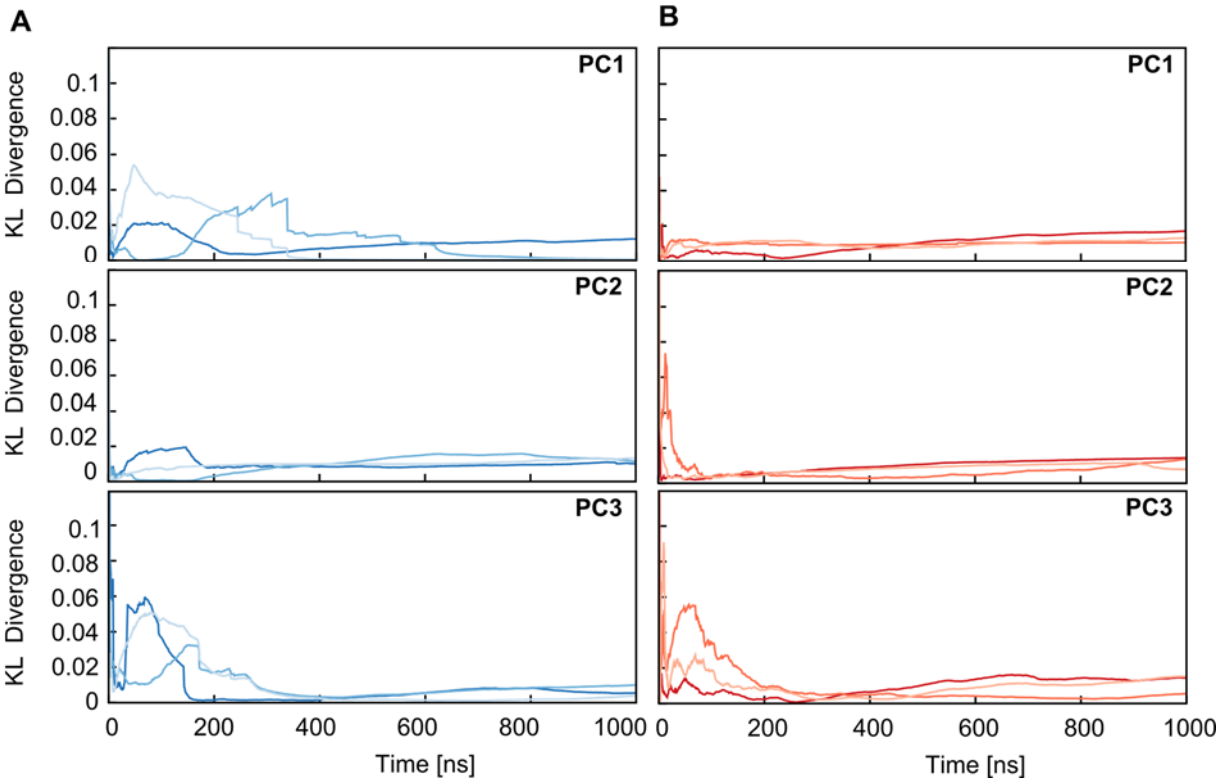

Fig S2: Convergence of internal motions in unbiased MD simulations.

Kullback-Leibler (KL) divergence[3] as a parameter to evaluate the convergence of the three independent MD simulations of Leu33 (HPA-1a) (**A**) and Pro33 (HPA-1b) (**B**). The KL divergence was computed for pair-wise comparisons of replicates of MD simulations in terms of histograms describing the projection of snapshots onto the given principal component (PC). The principal component analysis was performed on all the C_α atoms after alignment onto the β-propeller and βA domains. Lines colored in three different shades of blue and three different shades of red are used to represent the Leu33 (**A**) and Pro33 (**B**) isoforms, respectively.

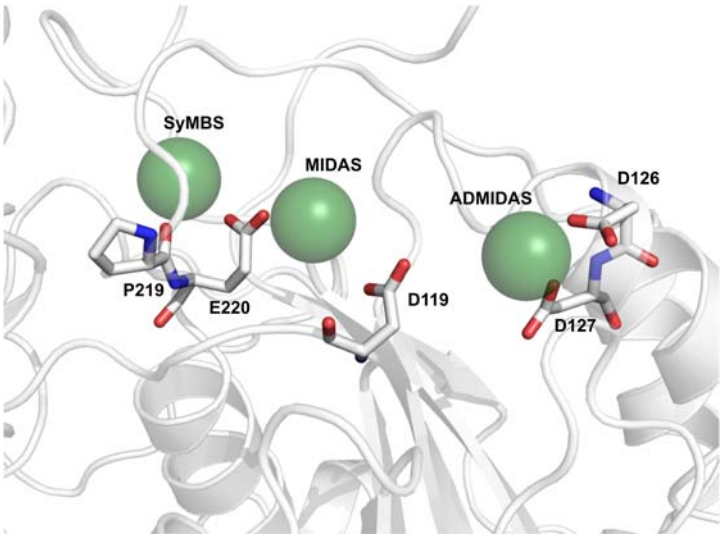

Fig S3: Metal ion binding sites

Close-up view of the metal binding sites within the βA domain. Metal ions are depicted as green spheres and labeled. Residues projecting from the βA domain (in cartoon drawing) involved in the metal coordination are shown in ball and sticks representation and labeled.

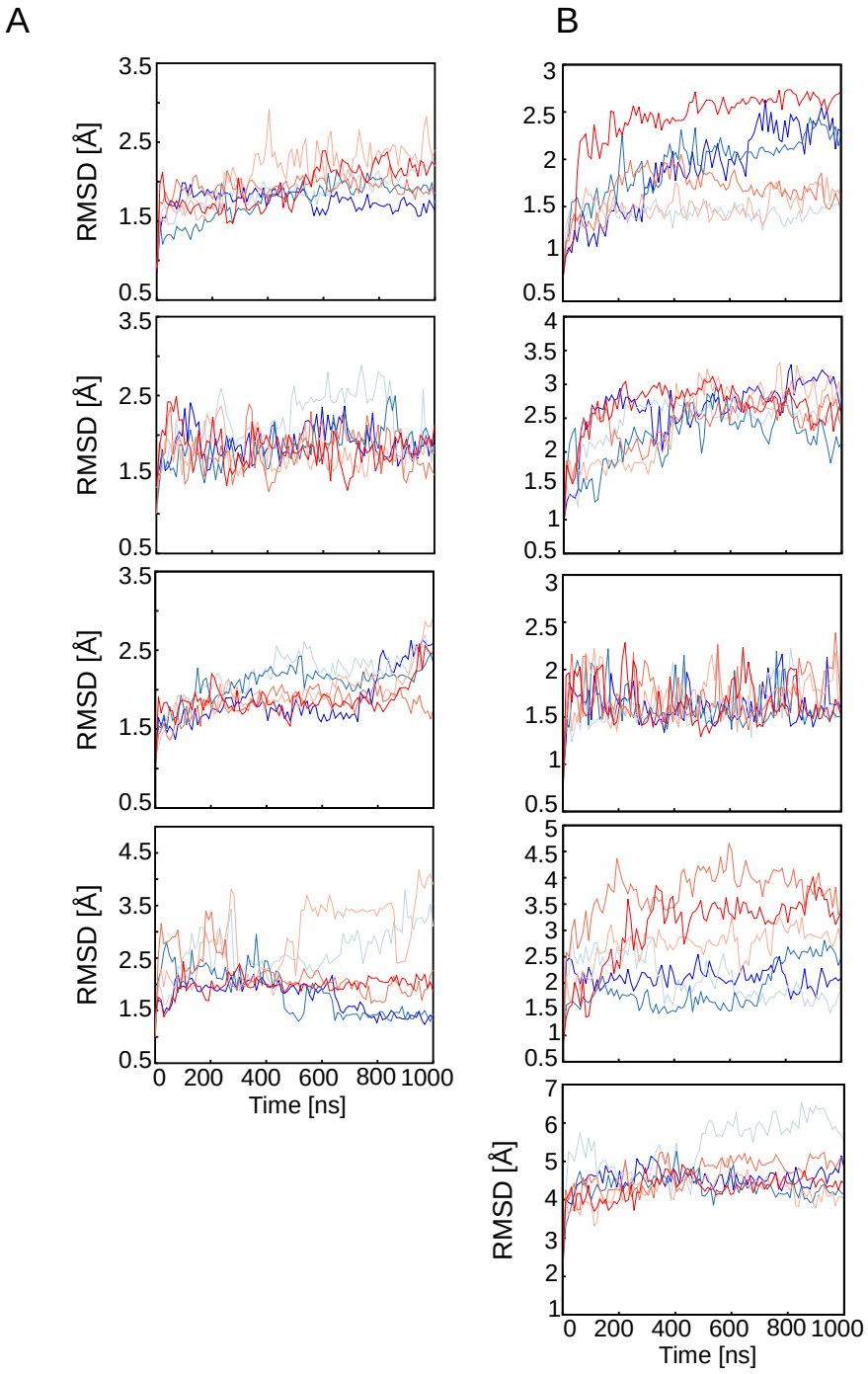

Fig. S4: Internal changes of $\alpha_{IIb}\beta_3$ domains: RMSD profiles.

RMSD of the C_α atoms of each domain of $\alpha_{IIb}\beta_3$ as a function of time with respect to the starting structure after a mass-weighted superimposition on the respective domain. From top to bottom, **(A)** the RMSD of the propeller domain, thigh domain, calf-1 and calf-2 domains is depicted, as is **(B)** the RMSD of the βA domain, hybrid domain, PSI domain, EGF block, and β-tail domains. Three different shades of blue and three different shades of red are used to represent the Leu33 and Pro33 isoforms, respectively.

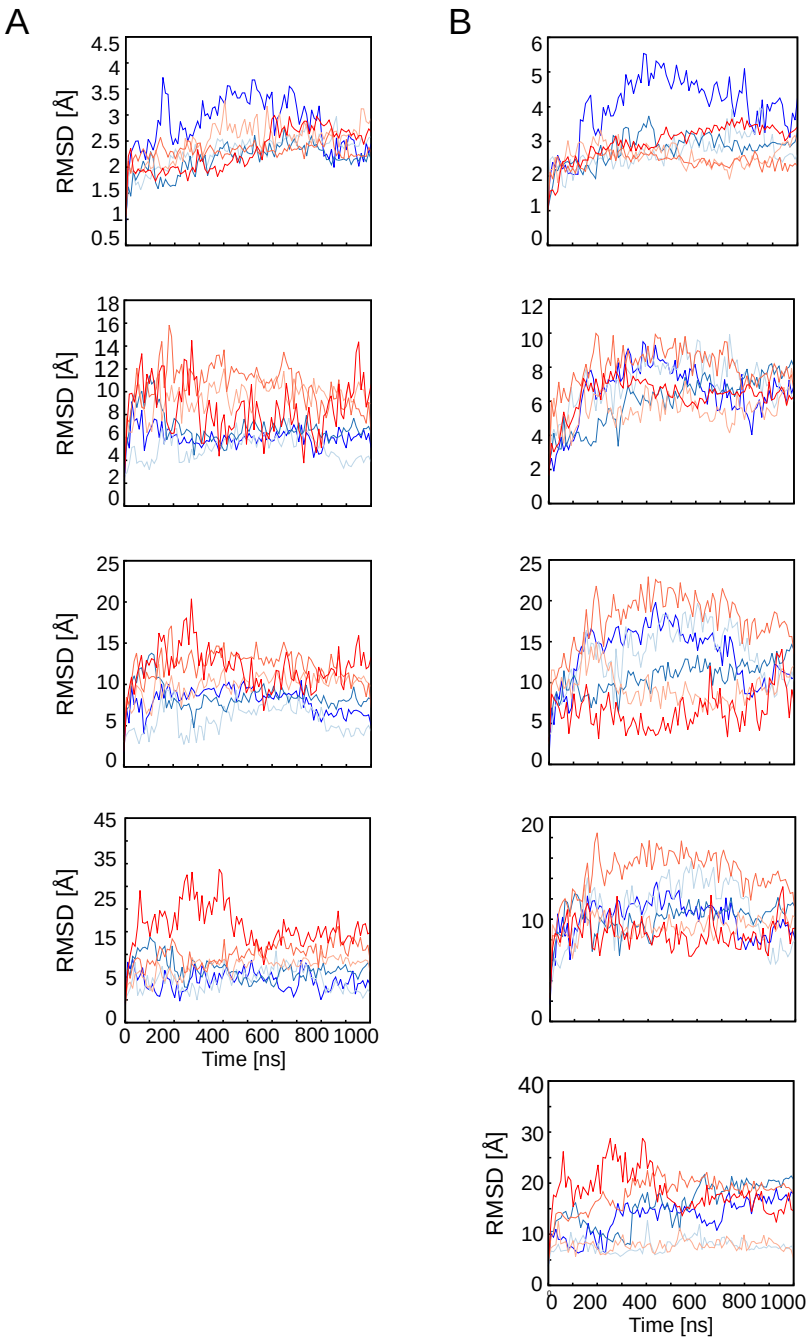

Fig. S5: Global changes of $\alpha_{IIb}\beta_3$ domains: RMSD profiles.

RMSD of the Cα atoms of each domain of $\alpha_{IIb}\beta_3$ as a function of time with respect to the starting structure after a mass-weighted superimposition on the head part (propeller domain and βA domain). From top to bottom, **(A)** the RMSD of the propeller domain, thigh domain, calf-1 and calf-2 domains is shown, as is **(B)** the RMSD of the βA domain, hybrid domain, PSI domain, EGF block, and β-tail domain. Three different shades of blue and three different shades of red are used to represent the Leu33 and Pro33 isoforms, respectively.

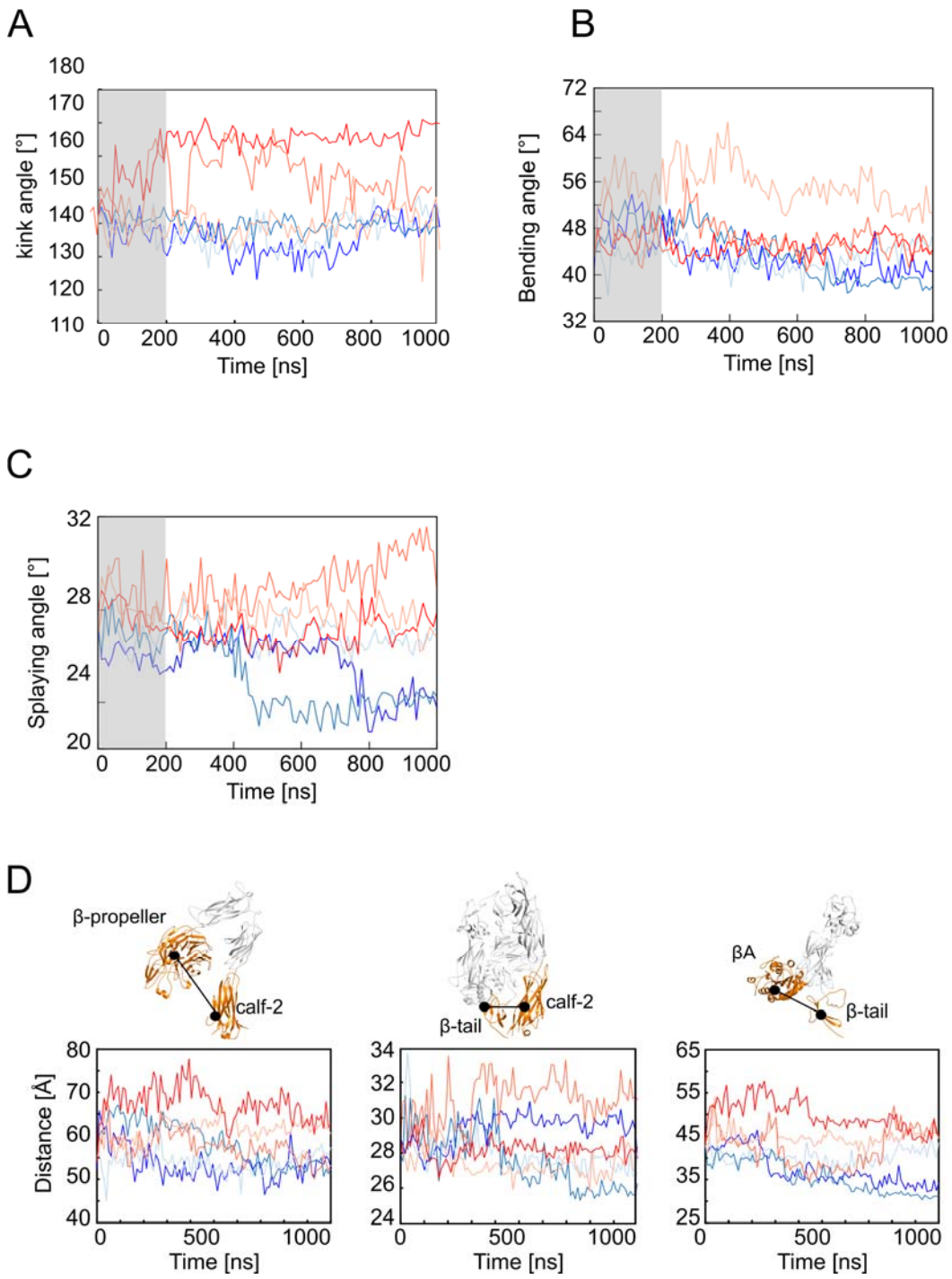

Fig. S6: Time series of geometric parameters.

(A, B, C) Time evolution of the kink angle, bending angle, and splaying angle defined as in the Methods section. Blue and red lines are used for the Leu33 (HPA-1a) isoform and Pro33 (HPA-1b) isoform, respectively. **(D)** Time evolution of the distances indicated in panel D. Above each panel, the initial structure of the respective MD simulations is depicted in cartoon representation. Domains involved in the measurements are labeled and highlighted in orange; the black line indicates the calculated distance between the COM of the domains (shown in black circles). Lines in color code as in panels (A)-(C).

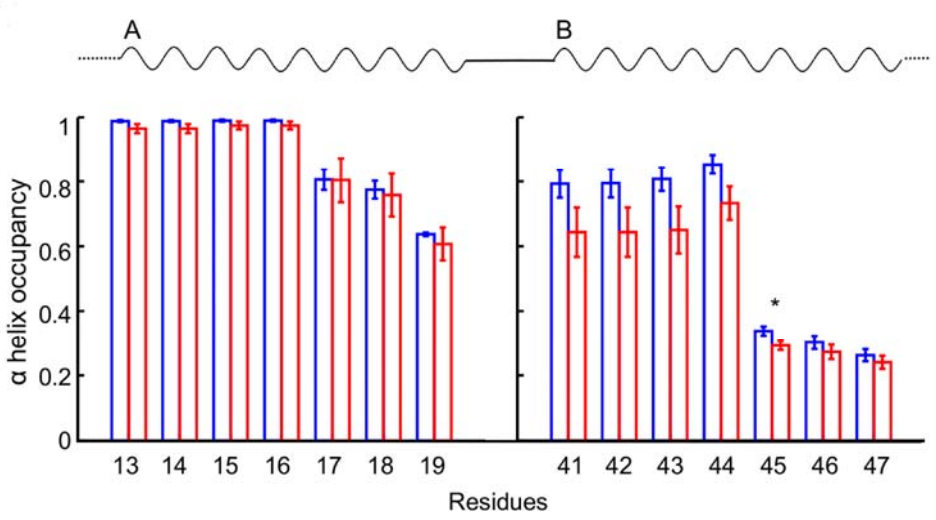

Fig. S7: Secondary structure analysis.

Normalized distribution of the helix content of **(A)** residues Cys13 to Met19 and **(B)** residues Leu40 to Asp47. Mean values calculated over three MD simulations are given, with error bars indicating SEM. The star indicates $p = 0.1$ for the difference. Blue and red colors represent the Leu33 and Pro33 isoforms, respectively.

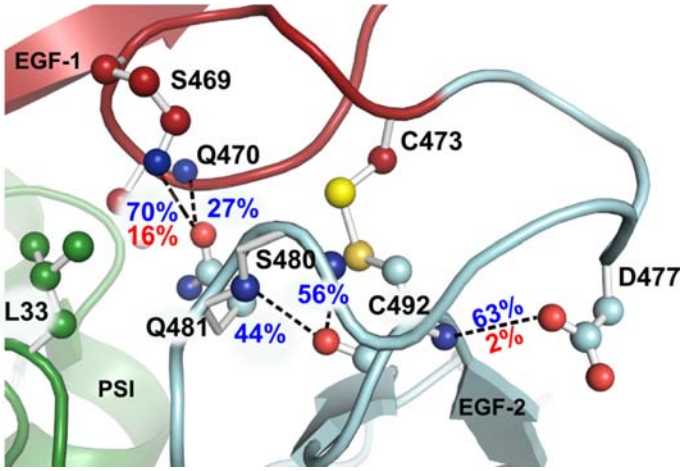

Fig. S8: Hydrogen bond network.

Mean occupancy of hydrogen bonds during three MD simulations each for the Leu33 (HPA-1a) and Pro33 (HPA-1b) isoform shown as labels next to the hydrogen bond marked by black dashed lines in the closest-to-average structure calculated from one simulation of the Leu33 (HPA-1a) isoform; occupancy values < 1% are not reported. For the sake of clarity, only the PSI (green), EGF-1 (firebrick), and EGF-2 (marine) domains of $\alpha_{IIb}\beta_3$ are shown. Residues Leu33 (PSI domain), Ser469-Gln470-Cys473 (EGF-1 domain), and Asp477-Ser480-Gln481-Cys492 (EGF-2 domain) are depicted in ball-and-sticks representation.

Supplemental References

1. Unkelbach, K., Kalb, R., Santoso, S., Kroll, H., Mueller-Eckhardt, C., and Kiefel, V. (1995) Genomic RFLP typing of human platelet alloantigens Zw(PlA), Ko, Bak and Br (HPA-1, 2, 3, 5). *Br. J. Haematol.* **89**, 169-176
2. Nauck, M. S., Gierens, H., Nauck, M. A., Marz, W., and Wieland, H. (1999) Rapid genotyping of human platelet antigen 1 (HPA-1) with fluorophore-labelled hybridization probes on the LightCycler. *Br. J. Haematol.* **105**, 803-810
3. Kunkel, T. A. (1985) Rapid and efficient site-specific mutagenesis without phenotypic selection. *Proc. Natl. Acad. Sci. U. S. A.* **82**, 488-492
4. Kim, M., Carman, C. V., and Springer, T. A. (2003) Bidirectional transmembrane signaling by cytoplasmic domain separation in integrins. *Science* **301**, 1720-1725
5. Galindo-Murillo, R., Roe, D. R., and Cheatham, T. E., 3rd. (2015) Convergence and reproducibility in molecular dynamics simulations of the DNA duplex d(GCACGAACGAACGAACGC). *Biochim. Biophys. Acta* **1850**, 1041-1058